U.S. ARMY COMBAT CAPABILITIES DEVELOPMENT COMMAND
CHEMICAL BIOLOGICAL CENTER

ABERDEEN PROVING GROUND, MD 21010-5424

CCDC CBC-TR-1601

Vapor Pressures of 2,4,6-Trimethyl-1,3,5-triazine (TMTZ) and 2,4,6-Trimethoxy-1,3,5-triazine (TMoxTZ)

Ann Brozena
James H. Buchanan
Eric J. Bruni

RESEARCH AND TECHNOLOGY DIRECTORATE

David E. Tevault

JOINT RESEARCH AND DEVELOPMENT, INC.
Belcamp, MD 21017-1552

December 2019

Disclaimer

The findings in this report are not to be construed as an official Department of the Army position unless so designated by other authorizing documents.

REPORT DOCUMENTATION PAGE

Form Approved
OMB No. 0704-0188

1. REPORT DATE *(DD-MM-YYYY)*	**2. REPORT TYPE**	**3. DATES COVERED** *(From - To)*
XX-12-2019	Final	Oct 2005–Sep 2010

4. TITLE AND SUBTITLE
Vapor Pressures of 2,4,6-Trimethyl-1,3,5-triazine (TMTZ) and 2,4,6-Trimethoxy-1,3,5-triazine (TMoxTZ)

5a. CONTRACT NUMBER

5b. GRANT NUMBER

5c. PROGRAM ELEMENT NUMBER

6. AUTHOR(S)
Brozena, Ann; Buchanan, James H.; Bruni, Eric J. (CCDC CBC); and Tevault, David E. (JRAD)

5d. PROJECT NUMBER
CB3662

5e. TASK NUMBER

5f. WORK UNIT NUMBER

7. PERFORMING ORGANIZATION NAME(S) AND ADDRESS(ES)
Director, CCDC CBC, ATTN: FCDD-CBR-CP, APG, MD 21010-5424
Joint Research and Development, Inc. (JRAD); 4694 Millennium Drive, Suite 105, Belcamp, MD 21017-1552

8. PERFORMING ORGANIZATION REPORT NUMBER
CCDC CBC-TR-1601

9. SPONSORING / MONITORING AGENCY NAME(S) AND ADDRESS(ES)
Defense Threat Reduction Agency, Joint Science and Technology Office, 8725 John J. Kingman Road, MSC 6201, Fort Belvoir, VA 22060-6201

10. SPONSOR/MONITOR'S ACRONYM(S)
DTRA JSTO

11. SPONSOR/MONITOR'S REPORT NUMBER(S)

12. DISTRIBUTION / AVAILABILITY STATEMENT
Approved for public release: distribution unlimited.

13. SUPPLEMENTARY NOTES
U.S. Army Combat Capabilities Development Command Chemical Biological Center (CCDC CBC) was previously known as U.S. Army Edgewood Chemical Biological Center (ECBC).

14. ABSTRACT:
The vapor pressure of 2,4,6-trimethyl-1,3,5-triazine (TMTZ) was measured between 69 and 156 °C for the liquid phase by differential scanning calorimetry (DSC) and between –20 and 10 °C for the solid phase using vapor saturation. The data sets were harmonized by fitting the liquid-phase data to an unconstrained Antoine equation and the solid-phase data to a Clausius–Clapeyron equation anchored by the vapor pressure at the melting point based on the DSC data. The difference in slopes between the liquid- and solid-phase correlations at the melting point enables estimation of the heat of fusion of TMTZ. The vapor pressure of liquid-phase 2,4,6-trimethoxy-1,3,5-triazine (TMoxTZ) was measured by DSC. The solid-phase vapor pressure of TMoxTZ was estimated using a Clausius–Clapeyron equation, the vapor pressure at the melting point calculated from the DSC data, and the heat of fusion of TMTZ. The vapor pressures of TMTZ and TMoxTZ are compared to those of GB and VX, the most- and least-volatile classical chemical warfare nerve agents, respectively. Volatility, enthalpies of vaporization and sublimation, and entropy of vaporization were calculated for both compounds from correlation equations based on the vapor pressure data. The melting points of both compounds were determined by DSC.

15. SUBJECT TERMS
2,4,6-Trimethyl-1,3,5-triazine (TMTZ), CAS no. 823-94-9
2,4,6-Trimethoxy-1,3,5-triazine (TMoxTZ), CAS no. 877-89-4
Vapor pressure
Differential scanning calorimetry (DSC)
Vapor saturation
Entropy of vaporization
Antoine equation
Clausius–Clapeyron equation
Volatility
Enthalpy of vaporization
Enthalpy of sublimation
Melting point

16. SECURITY CLASSIFICATION OF:			**17. LIMITATION OF ABSTRACT**	**18. NUMBER OF PAGES**	**19a. NAME OF RESPONSIBLE PERSON**
a. REPORT	**b. ABSTRACT**	**c. THIS PAGE**			Renu B. Rastogi
U	U	U	UU	32	**19b. TELEPHONE NUMBER** *(include area code)* (410) 436-7545

Blank

PREFACE

The work described in this report was funded by the Defense Threat Reduction Agency, Joint Science and Technology Office (Fort Belvoir, VA), project number CB3662. The work was performed between October 2005 and September 2010.

At the time this work was performed, the U.S. Army Combat Capabilities Development Command Chemical Biological Center (CCDC CBC) was known as the U.S. Army Edgewood Chemical Biological Center (ECBC). The data reported herein are documented in ECBC notebooks 99-0095, 06-0114, and 07-0072.

The use of either trade or manufacturers' names in this report does not constitute an official endorsement of any commercial products. This report may not be cited for purposes of advertisement.

This report has been approved for public release.

Acknowledgments

The authors acknowledge the following individuals from CCDC CBC for their assistance with the execution of this technical program:

- Dr. Fu-Lian Hsu for synthesizing the 2,4,6-trimethyl-1,3,5-triazine (TMTZ) used in this work;
- Mr. Kenneth Sumpter for determining the purity of the TMTZ used in this work; and
- Mr. Leonard Buettner for technical assistance.

Blank

CONTENTS

FIGURES

TABLES

VAPOR PRESSURES OF 2,4,6-TRIMETHYL-1,3,5-TRIAZINE (TMTZ) AND 2,4,6-TRIMETHOXY-1,3,5-TRIAZINE (TMoxTZ)

1. INTRODUCTION

Knowledge of the physical properties of materials is necessary to understand and accurately predict their behavior in the environment as well as in the laboratory. Vapor pressure is an important physical property for a wide variety of chemical defense-related applications, including evaluating toxicological properties and routes of entry, estimating persistence, assessing the efficiency of air filtration systems, predicting downwind time–concentration profiles after dissemination, and generating controlled challenge concentrations for detector testing.

The U.S. Army Edgewood Chemical Biological Center (ECBC; now known as the U.S. Army Combat Capabilities Development Command Chemical Biological Center; Aberdeen Proving Ground, MD) has a long history of interest in the thermophysical properties of chemical warfare agents (CWAs) and their precursors, degradation products, and simulants.[1–10] This report documents vapor pressure measurements, correlations, and thermodynamic properties derived from vapor pressure data for two compounds that may be considered candidate vapor pressure simulants for the classical nerve agents isopropyl methylphosphonofluoridate (GB or sarin) and *O*-ethyl-*S*-(2-diisopropylaminoethyl) methylphosphonothiolate (VX). The structures, chemical names, acronyms, formulas, Chemical Abstracts Service (CAS) registry numbers, and molecular weights (MWs) for the subject compounds are provided in Figure 1. Vapor pressure was determined using two modified ASTM International methods described herein; differential scanning calorimetry (DSC) measurements were performed at high temperatures for both compounds, and the vapor saturation method was used in the ambient temperature range for TMTZ.

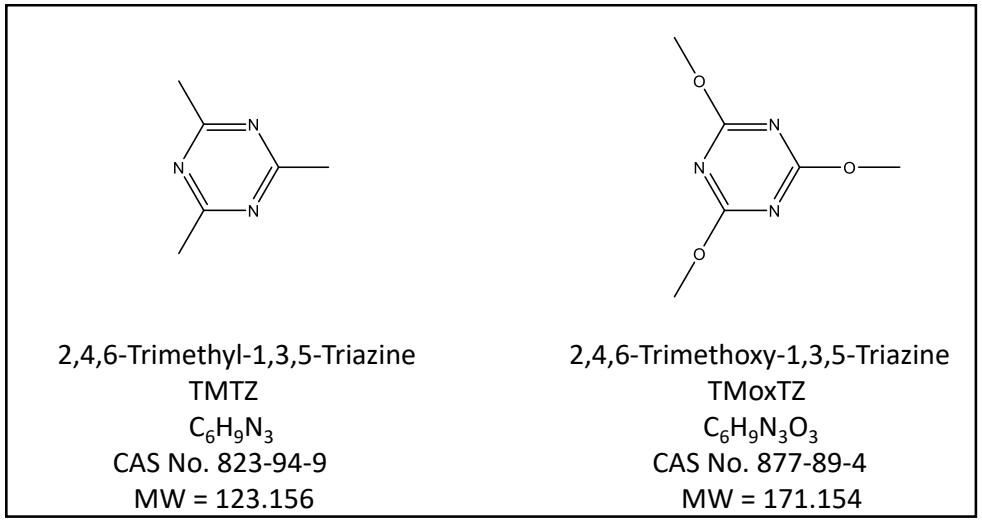

Figure 1. Structures, chemical names, acronyms, formulas, CAS numbers, and molecular weights of title compounds.

2. EXPERIMENTAL PROCEDURES

2.1 Materials

The sources and purities of the materials used in the current work are listed in Table 1. Both materials are solid at ambient temperature.

Table 1. Sample Information for Title Compounds

Compound	Method	Purity (%)	Source
TMTZ	DSC	99.9	Agent Chemistry Branch, ECBC
	Vapor saturation		
TMoxTZ	DSC	98.0	Aldrich Chemical Company (Milwaukee, WI)

2.2 Methods

2.2.1 DSC Procedure

DSC measurements were performed on both title compounds using TA Instruments (New Castle, DE) differential scanning calorimeters; a model 910 was used for TMoxTZ, and a model Q10P was used for TMTZ. The measurements were carried out in accordance with ASTM International method E 1782, *Standard Test Method for Determining Vapor Pressure by Thermal Analysis*.[11] This DSC pinhole method and instrumentation have been described in detail in a previous publication.[8]

2.2.2 Vapor Saturation Procedure

Vapor saturation measurements were performed for TMTZ in accordance with ASTM E 1194, *Standard Test Method for Vapor Pressure*,[12] using a vapor generator filled with glass beads. The system is identified in this report as the glass-bead vapor generator (GBVG).

The GBVG was constructed using a custom-designed, plastic-coated, borosilicate glass cell with a 4.8 cm inner diameter and a 6.9 cm bed depth (Glassblowers, Inc.; Turnersville, NJ). The glass cell was filled with 4 mm diameter spherical borosilicate glass beads, as shown in Figure 2. After the GBVG was assembled, the inner walls were rinsed several times with dichloromethane (HPLC grade, lot no. MKBG5835V; Aldrich Chemical Co., Inc.; Milwaukee, WI). TMTZ (235 mg) was dissolved in 17.55 mL of dichloromethane. This 1.00 wt % solution was then transferred to the GBVG via the inlet arm. Solvent rinses were used to wash residual TMTZ into the generator. Additional solvent was added until the solution level reached the top of the glass beads.

Solvent removal was accomplished using a technique previously described[13] and briefly discussed here. A slight vacuum was applied to the exit arm of the GBVG using a suitable pressure controller. The gradual reduction from ambient pressure to 200 Torr over 20–30 min allowed the TMTZ solution to be mixed during the slow solvent removal. This process was closely monitored to ensure that the bubbling of the solvent in the beads did not become too vigorous and thereby cause splashing onto the walls. The solvent removal process took approximately 4 h.

To prepare the vapor generator for use, it was conditioned for approximately 16 h using a dry nitrogen (dew point lower than –70 °C) flow with a 25.0 mL/min rate at 22.5 °C. This process purged the residual solvent and TMTZ from the outlet arm. Once conditioned, the generator was submerged in a circulating water–ethylene glycol bath (Neslab RTE-740; Newington, NH), so that its temperature could be carefully controlled (±0.1 °C) for vapor pressure measurements. The bath temperature was measured using calibrated thermometers (ERTCO; West Paterson, NJ). Ambient pressure was measured periodically during each run using a Nova mercury barometer (Princo Instruments, Inc.; Southampton, PA). All barometer readings were corrected for temperature and latitude according to the manufacturer's instructions and were accurate to ~13 Pa. The vapor generator was then integrated into the vapor pressure test system via a heated (100 °C), Sulfinert-treated, stainless steel tube (Restek Corp. [now SilcoTek]; Bellefonte, PA). Dry nitrogen carrier gas (25.0 mL/min) was introduced via the side arm (inlet) of the generator and passed through the thin-film coating of the TMTZ-wetted surfaces of the glass beads. This produced a TMTZ vapor concentration equal to the vapor pressure of TMTZ at the temperature of the water bath. The chemical stream exited the center arm (outlet) of the vapor generator and was transferred first to the ACEM model 900 unit (Dynatherm Analytical Instruments, Inc.; Kelton, PA, later acquired by CDS Analytical; Oxford, PA) for analyte concentration and then to a Hewlett-Packard model 5890 series II gas chromatograph (GC) equipped with a flame ionization detector (FID), as described in a previous report from our laboratory.[8] All ACEM 900 and GC–FID operating conditions in the current work were identical to those used in the previous work except for the column oven temperature profile. For TMTZ, the column oven was programmed to increase from 50 to 200 °C at 15 °C/min. This procedure produced a symmetrical TMTZ peak at 3.6 min, which corresponds to an elution temperature of 104 °C.

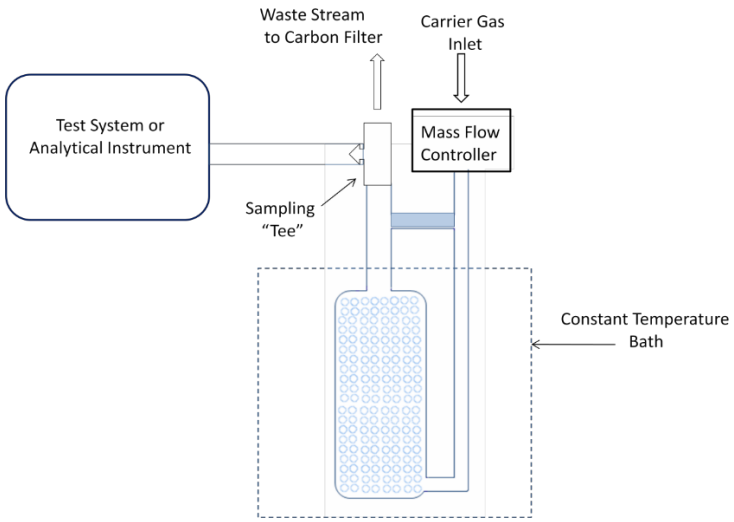

Figure 2. Glass-bead vapor generator (GBVG).

The GC was calibrated by injecting known masses of TMTZ and measuring the FID response. The resulting data were linear with a regression coefficient (R^2) of 0.993. For each vapor pressure experiment, a precisely measured volume of GBVG effluent was passed through the concentrator and into the calibrated GC to determine the mass of TMTZ in the sample. The vapor pressure was then determined by use of the ideal gas law as previously described.[8] Each vapor pressure data point represents the average of between 5 and 15 individual measurements. Carrier gas flow rate was quantified using a calibrated model FC-280 mass-flow controller (Tylan General; Austin, TX, later acquired by Brooks Instrument; Hatfield, PA). Confirmation that the vapor stream was saturated was demonstrated by doubling the flow rate through the GBVG and observing that no measurable change occurred in the analyte concentration.

2.3 Data Analysis

2.3.1 Vapor Pressure

Vapor pressure data were correlated using the Clausius–Clapeyron equation (eq 1) or the Antoine equation (eq 2) by minimizing the sum of the squares of the differences between the logarithms of the measured and calculated vapor pressure values (least-squares method). An alternate metric that was explored in this work utilized the sum of the absolute values of the percent differences between the experimental data and the calculated values. This metric is identified herein as |%D|. These optimization methodologies have been discussed in recent publications.[14,15]

$$\ln(P) = a - b/T \quad (1)$$

$$\ln(P) = a - b/(c + T) \quad (2)$$

where P is vapor pressure in pascal; T is absolute temperature; and a, b, and c are correlation constants.

Vapor pressure correlations in the literature are given using a variety of units. Most commonly in the older literature, vapor pressure is reported in torr units (mmHg; abbreviated herein as p), and temperature is reported in Celsius (t). Currently, most journals require that authors provide pressure in pascal and temperature in kelvin. Conversion of the correlation constants to alternate units has been discussed in detail in previous publications from our laboratory.[9,16]

High-quality vapor pressure data measured over a wide range is characterized by negative curvature on a standard vapor pressure plot (ln P versus reciprocal temperature) that corresponds to decreasing enthalpy of vaporization with increasing temperature. An *unconstrained* Antoine fit (where the c correlation constant is not set to a specific value) accurately describes this negative curvature over an extended temperature range and will produce the best fit to the data by minimizing the sum of the squares of the differences of the logarithms of the measured and calculated vapor pressure values. However, depending on the quality and range of the experimental data, an Antoine fit may produce thermodynamically prohibited positive curvature or excessive negative curvature.

When an Antoine fit yields a correlation with unacceptable positive curvature ($c > 0$, $C > 273$), a Clausius–Clapeyron correlation is preferred. This type of fit has no curvature due to the assumption of constant enthalpy of vaporization as a function of temperature. A Clausius–Clapeyron correlation may also be indicated when the experimental temperature range is limited or in the case of excessive negative curvature.

In the case of excessive negative curvature, another alternative is a *constrained* Antoine fit with c set to –43. This approach was recommended by Thomson,[17] who found that "In many cases which have been studied, C lies between 220 and 240" (c = –53 to –33 for kelvin units) and suggested using C = 230 (c = –43) as a "good average value" for correlation of vapor pressure "for organic compounds which are liquid at room temperature". For all of our liquid data sets that were measured over wide ranges using two or more complementary methods, the observed c values range from –16 to –88 with an average of –56 and a standard deviation of 18.[18] This range substantially overlaps the range suggested by Thomson. Accurately correlating vapor pressure data as a function of temperature to permit interpolation within the experimental range and extrapolation beyond that range has been addressed in earlier reports from our laboratory.[16,18]

Harmonizing correlations of solid- and liquid-phase data for the same compound can be more challenging. Ideally, liquid and solid correlations will both have reasonably negative curvature, produce an accurate heat of fusion based on the change in slope at the melting point, and meet at the melting point. In cases where the agreement between the data sets is poor, the intersection of the correlations may be *anchored* by using the projected value at the melting point based on the more reliable data set to constrain the less reliable data set.

The appropriate correlation equations for the title compounds were selected based on data quality, breadth of the experimental temperature range, and in some cases, curvature of the data plots.

2.3.2 Enthalpy of Vaporization

Thermodynamic properties can be calculated from the vapor pressure correlation. The enthalpy of vaporization (ΔH_{vap}), in joules per mole, can be calculated from vapor pressure data by multiplying the derivative of eq 2 with respect to T by $R \times T^2$, as shown:

$$\Delta H_{vap} = d[\ln(P)]/dT \times RT^2 = b \times R \times [T/(c + T)]^2 \quad (3)$$

where b and c are eq 2 coefficients, and R is the gas constant (8.3144 J/mol K).

Equation 3 can also be used to calculate the enthalpy of sublimation for solids.

2.3.3 Volatility (Saturation Concentration)

The saturation concentration (C_{sat}), often referred to as volatility, in milligrams per cubic meter, is calculated as a function of temperature according to

$$C_{sat} = P \times MW/(R \times T) \quad (4)$$

where R is 8.3144 Pa m^3/mol K.

2.3.4 Entropy of Vaporization

The entropy of vaporization (ΔS_{vap}), in joules per mole kelvin, is calculated by dividing the enthalpy of vaporization at the normal boiling point (NBPt) by the NBPt, as shown in eq 5. Trouton's rule[19] states that this value should be near 21 cal/mol K (88 J/mol K).

$$\Delta S_{vap} = \Delta H_{vap}/NBPt \quad (5)$$

3. RESULTS

3.1 2,4,6-Trimethyl-1,3,5-triazine (TMTZ)

Six DSC experiments were carried out on liquid TMTZ from 31.1 Torr to atmospheric pressure. The specimens were loaded at room temperature as solids, and a pressure-independent melting endotherm was the initial event observed on each thermal curve. The mean melting point was determined to be 59.2 °C with a standard deviation of 0.5 °C for these data. Boiling endotherms were observed on each thermal curve following melting, and these liquid vapor pressure data points extended from 69 to 156 °C. The boiling endotherms were sharp and showed no indication of degradation over the range studied.

Four data points were measured for solid TMTZ, in accordance with the vapor saturation method, using the GBVG from –20 to 10 °C.

The liquid-phase DSC data were fitted to an unconstrained Antoine equation that yielded acceptable negative curvature (c = –84). The solid-phase data were initially correlated using an unconstrained Antoine fit.[14] This approach resulted in good agreement between the data sets at the melting point (2362 vs 2557 Pa based on the DSC data); however, unacceptable positive curvature suggests that the solid-phase data are problematic.

A second attempt to correlate the saturator data to an Antoine equation using the b optimization method[14,15] with the |%D| metric resulted in a good fit to the experimental data and a reasonable c constant (–28); however, this fit produced poor agreement with the projected value at the melting point based on the DSC data (1502 vs 2557 Pa). As a result, this correlation was abandoned.

The third attempt to correlate the solid-phase data, using a Clausius–Clapeyron correlation (c = 0), resulted in a fit that was similar to the second, with a calculated vapor pressure of 1589 Pa at the melting point. This correlation was also rejected due to poor agreement with the projected value at the melting point based on the DSC data.

In light of these observations, we chose to fit the solid-phase TMTZ vapor pressure data using a Clausius–Clapeyron correlation anchored to the DSC value at the melting point to harmonize the data.[15]

The experimental DSC and saturator data for TMTZ are listed in Table 2. The resulting correlation equations for both phases are given at the bottom of Table 2 in torr and pascal units. Values calculated at the experimental temperatures from the listed equations and the percent differences between the experimental and calculated values are also provided. The agreement between the DSC experimental data and the calculated values is excellent. The saturator data agreement is not nearly as good, which again supports the notion of unknown experimental error in those data.

The DSC data and resulting Antoine equation correlation for liquid-phase TMTZ are illustrated in Figure 3.

Table 2. Experimental Data and Calculated Vapor Pressure Values for Solid- and Liquid-Phase TMTZ

Temperature (°C)	Experimental Vapor Pressure		Calculated Vapor Pressure		Difference* (%)
	(Torr)	(Pa)†	(Torr)	(Pa)	
Saturator – Solid Phase					
–20.0	1.086×10^{-2}	1.448×10^{0}	9.678×10^{-3}	1.290×10^{0}	12.23
–10.0	3.381×10^{-2}	4.508×10^{0}	3.247×10^{-2}	4.330×10^{0}	4.12
0.0	8.858×10^{-2}	1.181×10^{1}	9.973×10^{-2}	1.330×10^{1}	–11.17
10.0	2.507×10^{-1}	3.342×10^{1}	2.829×10^{-1}	3.772×10^{1}	–11.40
DSC* – Liquid Phase					
68.87	3.11×10^{1}	4.148×10^{3}	3.134×10^{1}	4.179×10^{3}	–0.75
80.11	5.40×10^{1}	7.198×10^{3}	5.308×10^{1}	7.076×10^{3}	1.72
87.66	7.34×10^{1}	9.791×10^{3}	7.381×10^{1}	9.840×10^{3}	–0.50
106.35	1.540×10^{2}	2.053×10^{4}	1.553×10^{2}	2.071×10^{4}	–0.86
120.66	2.593×10^{2}	3.457×10^{4}	2.584×10^{2}	3.444×10^{4}	0.36
155.94	7.570×10^{2}	1.009×10^{5}	7.566×10^{2}	1.009×10^{5}	0.05
Solid phase	$\ln(P) = 32.11227 - 8064.708/T$ $\log(p) = 11.82128 - 3502.458/(t + 273.15)$				
Liquid phase	$\ln(P) = 20.96337 - 3260.028/(T - 83.81176)$ $\log(p) = 6.979372 - 1415.812/(t + 189.3382)$				

*$100 \times (P_{exptl} - P_{calc})/P_{calc}$, where P_{exptl} is experimental vapor pressure, and P_{calc} is calculated vapor pressure.

†Experimental Pa values were calculated from torr values.

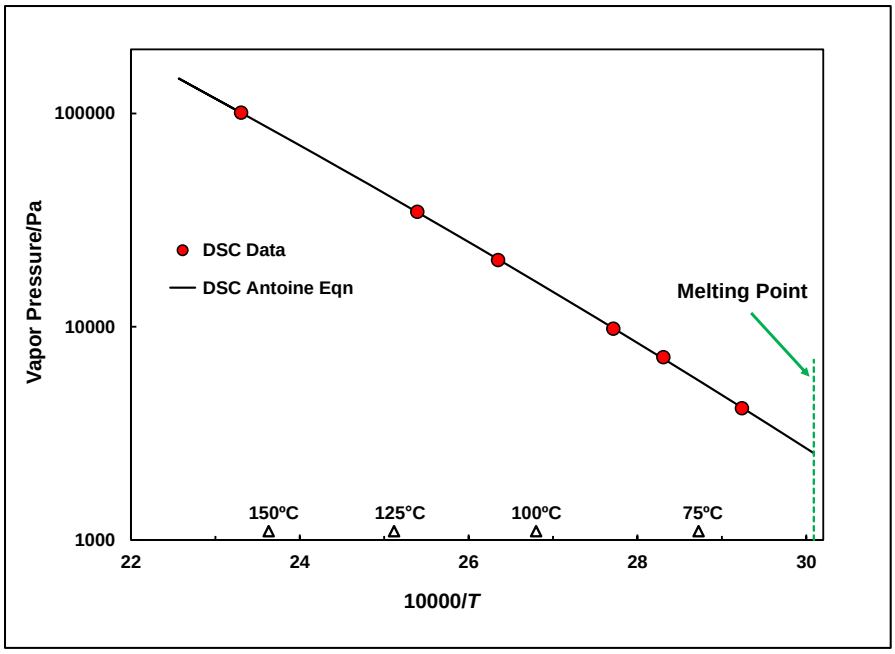

Figure 3. DSC data and Antoine equation correlation for liquid-phase TMTZ.

The solid-phase data and a comparison of the candidate correlations for TMTZ are illustrated in Figure 4. Figure 5 shows the experimental vapor pressure data, the Antoine (liquid-phase), and the recommended anchored Clausius–Clapeyron (solid-phase) correlations.

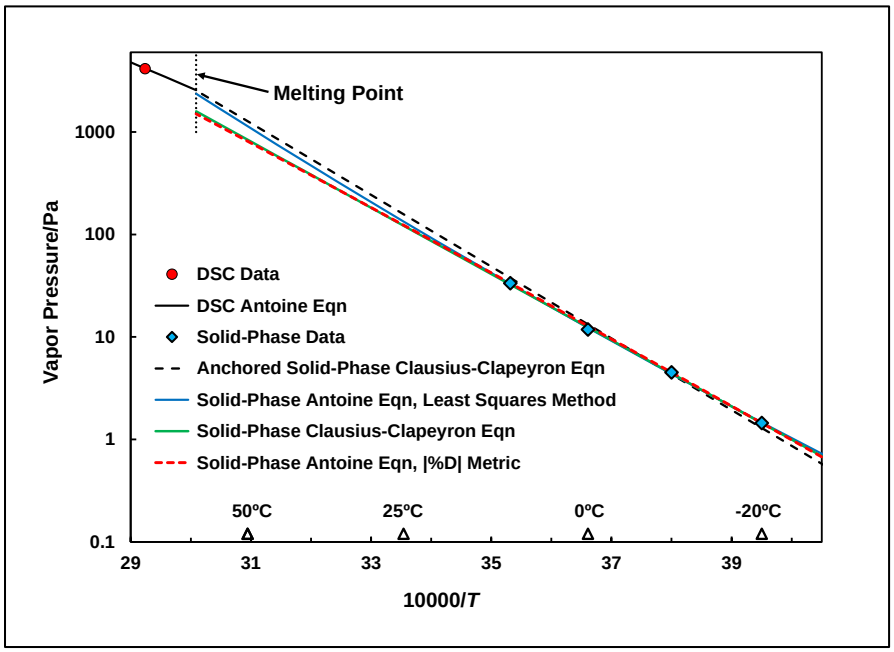

Figure 4. GBVG data and candidate correlations for solid-phase TMTZ.

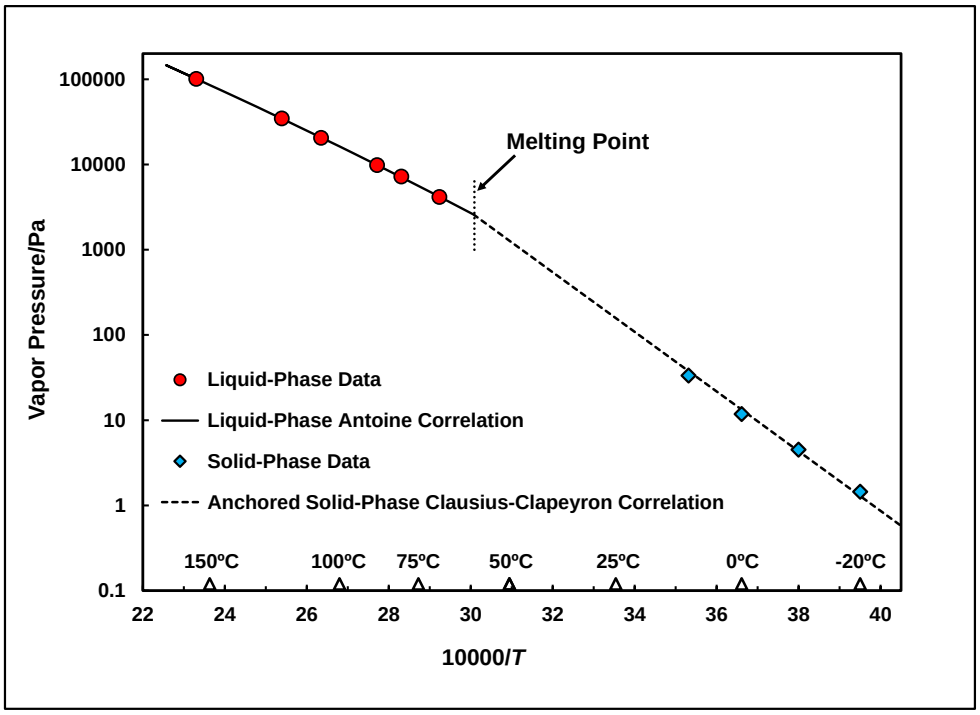

Figure 5. TMTZ vapor pressure data, correlations, and melting point.

Table 3 lists the calculated vapor pressures in torr and pascal units, volatility, and enthalpy of volatilization (sublimation for solid and vaporization for liquid) values between t = –20 °C and the extrapolated NBPt, 156.10 °C, based on the correlations at the bottom of Table 2. The enthalpy of fusion can be calculated from the difference between the enthalpies of sublimation and vaporization at the melting point and was determined to be 18.58 kJ/mol. The enthalpy of sublimation is constant over the solid-phase temperature range due to the use of the Clausius–Clapeyron equation for the data correlation. Based on the DSC data, the entropy of vaporization is 97.5 J/mol K.

Table 3. Calculated Vapor Pressure, Volatility, and Enthalpies of Sublimation and Vaporization for TMTZ at Selected Temperatures

Temperature (°C)	Vapor Pressure		Volatility (mg/m^3)	$\Delta H_{volatilization}$ (kJ/mol)*
	(Torr)	(Pa)		
Solid Phase				
–20	9.678×10^{-3}	1.290×10^{0}	7.549×10^{1}	67.05
–10	3.247×10^{-2}	4.330×10^{0}	2.437×10^{2}	
0	9.973×10^{-2}	1.330×10^{1}	7.210×10^{2}	
10	2.829×10^{-1}	3.772×10^{1}	1.973×10^{3}	
20	7.475×10^{-1}	9.966×10^{1}	5.036×10^{3}	
25	1.186×10^{0}	1.581×10^{2}	7.853×10^{3}	
30	1.852×10^{0}	2.470×10^{2}	1.207×10^{4}	
40	4.332×10^{0}	5.775×10^{2}	2.732×10^{4}	
50	9.611×10^{0}	1.281×10^{3}	5.874×10^{4}	
59.2	1.918×10^{1}	2.557×10^{3}	1.140×10^{5}	
Liquid Phase				
59.2	1.918×10^{1}	2.557×10^{3}	1.140×10^{5}	48.47
60	2.000×10^{1}	2.667×10^{3}	1.186×10^{5}	48.39
70	3.312×10^{1}	4.415×10^{3}	1.906×10^{5}	47.46
80	5.281×10^{1}	7.041×10^{3}	2.953×10^{5}	46.60
90	8.146×10^{1}	1.086×10^{4}	4.430×10^{5}	45.81
100	1.219×10^{2}	1.626×10^{4}	6.453×10^{5}	45.08
110	1.777×10^{2}	2.369×10^{4}	9.156×10^{5}	44.41
120	2.526×10^{2}	3.368×10^{4}	1.269×10^{6}	43.78
130	3.514×10^{2}	4.685×10^{4}	1.721×10^{6}	43.20
140	4.791×10^{2}	6.387×10^{4}	2.290×10^{6}	42.66
150	6.414×10^{2}	8.551×10^{4}	2.993×10^{6}	42.15
156.10	7.600×10^{2}	1.013×10^{5}	3.496×10^{6}	41.85

*For the solid phase, the value is the enthalpy of sublimation; for the liquid phase, the values are the temperature-dependent enthalpies of vaporization.

3.2 2,4,6-Trimethoxy-1,3,5-triazine (TMoxTZ)

DSC measurements were attempted on both the solid and liquid phases of TMoxTZ from 0.6 Torr to atmospheric pressure. Seven experiments were performed on the solid phase between 0.6 and 7.5 Torr using a variety of pinhole sizes. All of the boiling endotherms were unacceptably broad; this was presumably due to poor thermal contact between the solid and the DSC pan.

Sixteen DSC experiments were performed on the liquid phase from 18 Torr to atmospheric pressure. A sharp, pressure-independent melting endotherm was the initial event observed on each of these thermal curves. The mean melting point from 12 experiments was determined to be 134.1 °C with a standard deviation of 0.4 °C. Fifteen of the curves yielded acceptably sharp boiling endotherms from 18.4 to 296.5 Torr, corresponding to boiling

temperatures of 148 to 230 °C, following melting. For the experiment at 296.5 Torr, the typically flat pre-boiling baseline started to rise. This suggested the onset of a thermal event other than boiling; however, an acceptable boiling endotherm followed. The atmospheric pressure thermal curve showed a broad exotherm before a broadened boiling endotherm. This result suggests the onset of decomposition, as the atmospheric pressure endotherm is usually the sharpest peak observed in a data set in the absence of thermal degradation. As a result, the atmospheric pressure point was not used for the correlation. The data generated from these experiments are listed in Table 4 in both torr and pascal units.

No saturator measurements were performed on TMoxTZ.

Our initial attempt to correlate the TMoxTZ DSC data using an unconstrained Antoine equation resulted in a large (negative) *c* constant, –183.3, which is characteristic of excessive negative curvature of the experimental data. Therefore, we constrained the liquid-phase correlation by using Thomson's suggested *c* value (–43). The resulting equation is given at the bottom of Table 4 in two pressure units, along with the values calculated at the experimental temperatures and the percent differences between experimental and calculated values. Figure 6 shows the liquid-phase experimental vapor pressure data and the constrained Antoine correlation.

Calculated values for vapor pressure in torr and pascal units, volatility, and enthalpy of vaporization between the melting point and normal boiling point are given in Table 5. The entropy of vaporization calculated on the basis of the TMoxTZ DSC data is 90.0 J/mol K.

Table 4. Experimental Data and Calculated Vapor Pressure Values for Liquid-Phase TMoxTZ

Temperature (°C)	Experimental Vapor Pressure		Calculated Vapor Pressure		Difference* (%)
	(Torr)	(Pa)†	(Torr)	(Pa)	
147.8	1.84×10^1	2.453×10^3	1.886×10^1	2.514×10^3	–2.43
150.4	2.03×10^1	2.706×10^3	2.100×10^1	2.800×10^3	–3.35
153.4	2.34×10^1	3.120×10^3	2.374×10^1	3.165×10^3	–1.44
157.0	2.73×10^1	3.640×10^3	2.744×10^1	3.658×10^3	–0.49
158.7	3.02×10^1	4.026×10^3	2.935×10^1	3.913×10^3	2.91
163.5	3.52×10^1	4.693×10^3	3.538×10^1	4.717×10^3	–0.51
166.0	3.97×10^1	5.293×10^3	3.893×10^1	5.190×10^3	1.98
172.1	5.01×10^1	6.679×10^3	4.891×10^1	6.521×10^3	2.43
188.2	8.96×10^1	1.195×10^4	8.653×10^1	1.154×10^4	3.55
199.8	1.300×10^2	1.733×10^4	1.271×10^2	1.695×10^4	2.28
209.0	1.711×10^2	2.281×10^4	1.700×10^2	2.266×10^4	0.67
212.4	1.898×10^2	2.530×10^4	1.886×10^2	2.515×10^4	0.61
216.1	2.097×10^2	2.796×10^4	2.109×10^2	2.812×10^4	–0.59
219.1	2.296×10^2	3.061×10^4	2.306×10^2	3.075×10^4	–0.44
229.5	2.965×10^2	3.953×10^4	3.114×10^2	4.152×10^4	–4.79
$\ln(P) = 23.60603 - 5962.661/(T - 43.0000)$ $\log(p) = 8.127065 - 2589.551/(t + 230.1500)$					

*$100 \times (P_{exptl} - P_{calc})/P_{calc}$, where P_{exptl} is experimental vapor pressure, and P_{calc} is calculated vapor pressure.

†Experimental Pa values were converted from torr values.

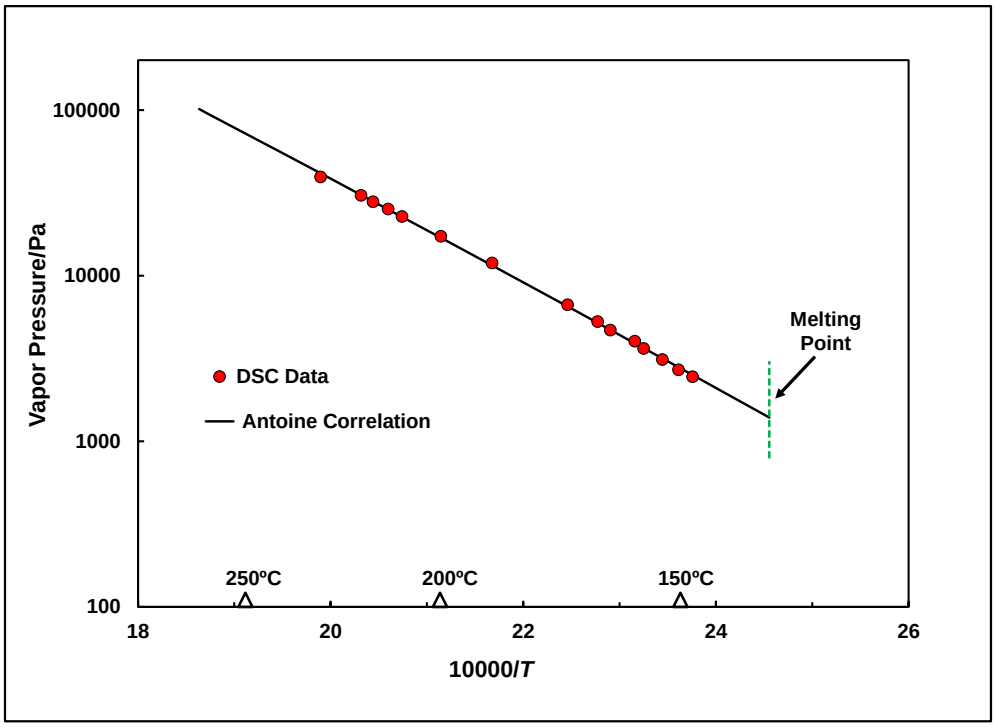

Figure 6. TMoxTZ experimental vapor pressure data and constrained (c = –43) Antoine equation correlation and melting point.

Table 5. Calculated Vapor Pressure, Volatility, and Enthalpy of Vaporization for Liquid TMoxTZ at Selected Temperatures

Temperature (°C)	Vapor Pressure		Volatility (mg/m^3)	ΔH_{vap} (kJ/mol)
	(Torr)	(Pa)		
134.1	1.042×10^1	1.389×10^3	7.021×10^4	61.97
140	1.352×10^1	1.803×10^3	8.984×10^4	61.76
150	2.066×10^1	2.755×10^3	1.340×10^5	61.43
160	3.088×10^1	4.118×10^3	1.957×10^5	61.11
170	4.525×10^1	6.033×10^3	2.802×10^5	60.80
180	6.507×10^1	8.676×10^3	3.941×10^5	60.52
190	9.197×10^1	1.226×10^4	5.450×10^5	60.24
200	1.279×10^2	1.706×10^4	7.420×10^5	59.98
210	1.753×10^2	2.337×10^4	9.956×10^5	59.74
220	2.368×10^2	3.157×10^4	1.318×10^6	59.50
230	3.158×10^2	4.211×10^4	1.723×10^6	59.27
240	4.160×10^2	5.547×10^4	2.225×10^6	59.06
250	5.418×10^2	7.224×10^4	2.842×10^6	58.85
260	6.980×10^2	9.307×10^4	3.593×10^6	58.66
263.45	7.600×10^2	1.013×10^5	3.887×10^6	58.59

4. DISCUSSION

The TMTZ DSC data may be characterized as having excellent agreement between experimental and calculated values with an acceptable *c* constant of –84. In addition, the lowest DSC data point is within 10 °C of the melting point, minimizing extrapolation of the correlation to the melting point. The entropy of vaporization for TMTZ indicated by the current DSC data, 97.5 J/mol K, is about 10% higher than predicted on the basis of Trouton's rule; however, Langmuir has observed that such a difference is common among larger molecules.[20] We have many data sets[16] that are consistent with Langmuir's observation. All of these factors give us confidence in the DSC data and the extrapolated value of the vapor pressure at the melting point.

Additional work to verify or refine the solid-phase TMTZ vapor pressure data is recommended on the basis of the experimental error suggested by the current results. Our hypothesis is that not enough time was allowed for the GBVG to achieve thermal equilibrium, which caused the actual temperatures to be different than indicated due to the high heat capacity and low thermal conductivity of the glass bead packing that was used.

The ability to calculate heat of fusion from the difference between the enthalpies of sublimation and vaporization at the melting point is limited to cases where vapor pressure data are available for both the liquid and solid phases. Comparison of the value calculated herein for TMTZ to an experimental value measured directly by other techniques would be useful.

The experimental vapor pressure data for TMoxTZ was limited to liquid-phase DSC measurements. The unconstrained Antoine fit of the data produced a large negative *c* constant of –183.3 and a significantly lower than anticipated calculated entropy of vaporization of 67.5 J/mol K. This low entropy value is a direct result of two effects. First, the greater curvature of the correlation resulted in a lower than expected slope of the vapor pressure curve and calculated enthalpy of vaporization at the boiling point; and second, the excessive curvature also produced a higher than expected boiling point. This low entropy value is inconsistent with Langmuir's observation and also suggests that the unconstrained Antoine fit is not the best representation of the data.

As a result, we have chosen to constrain the correlation by adopting Thomson's suggested *c* value (–43). This approach has the advantage of producing an entropy of vaporization of 90.0 J/mol K, which is very close to the value expected on the basis of Trouton's rule albeit at the expense of a slightly better agreement between experimental and calculated values.

The agreement between the experimental DSC vapor pressure data and calculated values for TMoxTZ is not as good as that observed for TMTZ. The principal reason is assumed to be the degradation of TMoxTZ at the higher pressures used in the current work. Efforts to use as many DSC data points as possible in the correlation may have resulted in inclusion of one or more points influenced by incipient decomposition. Another contributing factor may be DSC method-optimization efforts that occurred after the TMoxTZ work was completed but before the TMTZ work was performed.

Attempts to measure data for solid-phase TMoxTZ using DSC were unsuccessful as detailed herein. Nevertheless, ambient-temperature vapor pressure values for the solid may be estimated by assuming that the enthalpy of fusion for TMoxTZ is the same as that for TMTZ. In the absence of knowledge about how the enthalpy of sublimation varies with temperature, we have assumed that it remains constant, resulting in a Clausius–Clapeyron correlation to represent the solid-phase TMoxTZ vapor pressure. The equation and estimated vapor pressures from T = –40 °C to the melting point are provided in Table 6.

Table 6. Estimated Vapor Pressures for Solid TMoxTZ at Selected Temperatures, Enthalpy of Sublimation, and Clausius–Clapeyron Correlations

Temperature (°C)	P_{calc} (Torr)	P_{calc} (Pa)	Volatility (mg/m^3)	$\Delta H_{sublimation}$ (kJ/mol)
–40	2.009×10^{-7}	2.679×10^{-5}	2.365×10^{-3}	80.55
–20	5.355×10^{-6}	7.140×10^{-4}	5.806×10^{-2}	
0	8.825×10^{-5}	1.177×10^{-2}	8.867×10^{-1}	
20	9.922×10^{-4}	1.323×10^{-1}	9.289×10^{0}	
25	1.727×10^{-3}	2.303×10^{-1}	1.590×10^{1}	
30	2.952×10^{-3}	3.935×10^{-1}	2.672×10^{1}	
40	8.190×10^{-3}	1.092×10^{0}	7.178×10^{1}	
60	5.247×10^{-2}	6.995×10^{0}	4.322×10^{2}	
80	2.723×10^{-1}	3.631×10^{1}	2.116×10^{3}	
100	1.185×10^{0}	1.580×10^{2}	8.715×10^{3}	
120	4.439×10^{0}	5.918×10^{2}	3.099×10^{4}	
134.1	1.042×10^{1}	1.389×10^{3}	7.021×10^{4}	
$\ln(P) = 31.02519 - 9688.011/T$ $\log(p) = 11.34917 - 4207.450/(t + 273.15)$				

Figure 7 shows a comparison of the vapor pressure curves for the title compounds to those for VX[10] and GB,[21] which are prototypical low- and high-volatility classical CWAs, respectively. Note the changes in the slopes of the correlations for the title compounds at their melting points, whereas VX and GB are liquids throughout the range shown on the plot.

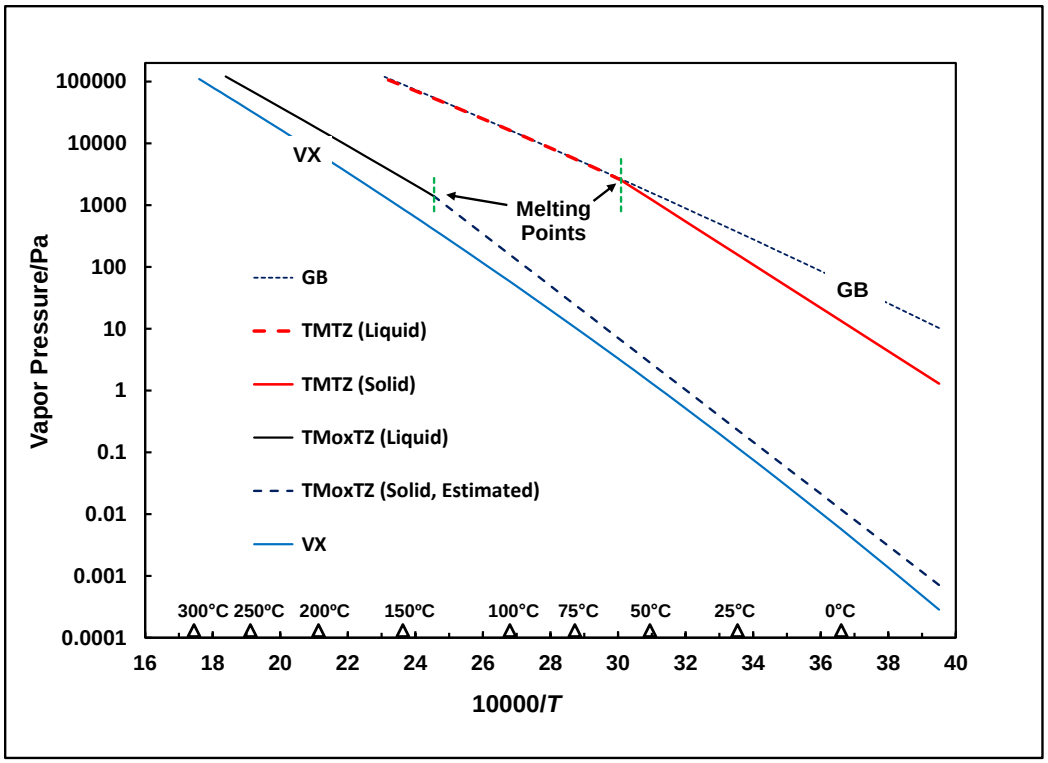

Figure 7. Comparison of the vapor pressures of TMTZ, TMoxTZ, VX, and GB.

5. CONCLUSIONS

This report describes measurement and analysis of the vapor pressures of the liquid and solid phases of TMTZ and the liquid phase of TMoxTZ. The melting points of both compounds were also determined. TMTZ is stable up to its normal boiling point of 156.1 °C, whereas TMoxTZ begins to show effects of thermal instability at about 220 °C. We were unable to measure vapor pressure data for TMoxTZ below its melting point, but we were able to estimate values based on the assumption that it has the same heat of fusion as TMTZ.

At temperatures above its melting point, the vapor pressure of TMTZ is the same as that of GB (the most volatile of the standard chemical warfare nerve agents) within our current experimental uncertainty. At temperatures below its melting point, the vapor pressure of TMTZ decreases more rapidly than that of GB, due to the change in slope at the melting point.

The estimated vapor pressure of solid-phase TMoxTZ is a factor of 2–3.5 higher than that of VX (the least volatile of the traditional chemical warfare nerve agents).

Blank

LITERATURE CITED

1. Felsing, W.A.; Arenson, S.B.; Kopp, F.J. A Method for Determining the Sulfur Monochloride Content of Mustard Gas-S_2Cl_2 Mixtures. *J. Ind. Eng. Chem*. **1920,** *12* (11), 1054–1056.

2. Thompson, T.G.; Kopp, F.J. Pressures Produced by the Action of Sulfur Monochloride upon β,β′-Dichloroethyl Sulfide. *J. Ind. Eng. Chem.* **1920,** *12* (11), 1056–1057.

3. Felsing, W.A.; Hunting, C.A.; Fell, S.D. The Melting Point of Mustard Gas. *J. Am. Chem. Soc*. **1948,** *70* (5), 1966.

4. *Report on Properties of War Gases, Volume I, G Agents*; Chemical Corps Board: Army Chemical Center, MD, 1956; UNCLASSIFIED Report (AD0108456).

5. Zeffert, B.M.; Coulter, P.B.; Tannenbaum, H. Properties, Interaction, and Esterification of Methylphosphonic Dihalides. *J. Am. Chem. Soc*. **1960,** *82* (15), 3843–3847.

6. Belkin, F.; Brown, H.A., Jr. *Vapor Pressure Measurements of Some Chemical Agents Using Differential Thermal Analysis, Part I*; EATR-4710; Edgewood Arsenal: Aberdeen Proving Ground, MD, 1973; UNCLASSIFIED Report (AD0525359).

7. Penski, E.C. Physical Chemistry Research at CBDCOM – Past and Future. In *Proceedings of the 1995 ERDEC Scientific Conference on Chemical and Biological Defense Research, 14–17 November 1995*; ERDEC-SP-043; U.S. Army Edgewood Research, Development and Engineering Center: Aberdeen Proving Ground, MD, 1996, 307–311; UNCLASSIFIED Report (ADA315812).

8. Butrow, A.B.; Buchanan, J.H.; Tevault, D.E. Vapor Pressure of Organophosphorus Nerve Agent Simulant Compounds. *J. Chem. Eng. Data* **2009,** *54* (6), 1876–1883.

9. Tevault, D.E.; Buchanan, J.H.; Buettner, L.C.; Matson, K.L. *Vapor Pressure of Cyclohexyl Methylphosphonofluoridate (GF)*; ECBC-TR-304; U.S. Army Edgewood Chemical Biological Center: Aberdeen Proving Ground, MD, 2009; UNCLASSIFIED Report (ADA503835).

10. Tevault, D.E.; Brozena, A.; Buchanan, J.H.; Abercrombie-Thomas, P.L.; Buettner, L.C. Thermophysical Properties of VX and RVX. *J. Chem. Eng. Data* **2012,** *57* (7), 1970−1977.

11. *Standard Test Method for Determining Vapor Pressure by Thermal Analysis;* ASTM E 1782; ASTM International: West Conshohocken, PA, 2014.

12. *Standard Test Method for Vapor Pressure;* ASTM E 1194; ASTM International: West Conshohocken, PA, 2017.

13. Jenkins, A.L.; Bruni, E.J.; Buettner, L.C.; Sohrabi, A.; Ellzy, M.W. *Vapor Pressure Determination of VM Using the Denuder–Liquid Chromatography–Mass Spectrometry Technique*; ECBC-TR-1278; U.S. Army Edgewood Chemical Biological Center: Aberdeen Proving Ground, MD, 2015, UNCLASSIFIED Report (ADA613614).

14. Brozena, A.; Davidson, C.E.; Ben-David, A.; Schindler, B.; Tevault, D.E. *Vapor Pressure Data Analysis and Statistics*; ECBC-TR-1422; U.S. Army Edgewood Chemical Biological Center: Aberdeen Proving Ground, MD, 2016; UNCLASSIFIED Report (AD1022530).

15. Tevault, D.E. *Vapor Pressure Data Analysis and Correlation Methodology for Data Spanning the Melting Point*; ECBC-CR-135; U.S. Army Edgewood Chemical Biological Center: Aberdeen Proving Ground, MD, 2013; UNCLASSIFIED Report (ADA592605).

16. Brozena, A.; Tevault, D.E. *Vapor Pressure Data and Analysis for Selected HD Decomposition Products: 1,4-Thioxane, Divinyl Sulfoxide, Chloroethyl Acetylsulfide, and 1,4-Dithiane*; ECBC-TR-1514; U.S. Army Edgewood Chemical Biological Center: Aberdeen Proving Ground, MD, 2018; UNCLASSIFIED Report (AD1053736).

17. Thomson, G.W. The Antoine Equation for Vapor-Pressure Data. *Chem. Re*v. **1946,** *38,* 1–39.

18. Brozena, A.; Abercrombie-Thomas, P.L.; Tevault, D.E. *Vapor Pressure Data and Analysis for Selected Organophosphorus Compounds, CMMP, DPMP, DMEP, and DEEP: Extrapolation of High-Temperature Data*; ECBC-TR-1507; U.S. Army Edgewood Chemical Biological Center: Aberdeen Proving Ground, MD, 2018; UNCLASSIFIED Report (AD1049398).

19. Alberty, R.A.; Daniels, F. *Physical Chemistry*, 5th ed.; John Wiley & Sons: New York, 1979, p 99.

20. Langmuir, I. Vapor Pressures, Evaporation, Condensation and Adsorption. *J. Am. Chem. Soc.* **1932,** *54* (7), 2798–2832.

21. Buchanan, J.H.; Sumpter, K.B.; Abercrombie, P.L.; Tevault, D.E. *Vapor Pressure of GB;* ECBC-TR-686; U.S. Army Edgewood Chemical Biological Center: Aberdeen Proving Ground, MD, 2009; UNCLASSIFIED Report (ADA500820).

ACRONYMS AND ABBREVIATIONS

ΔH_{vap}	enthalpy of vaporization
ΔS_{vap}	entropy of vaporization
a, b, c	vapor pressure fit constants
CAS	Chemical Abstracts Service
C_{sat}	saturation concentration or volatility
CWA	chemical warfare agent
|%D|	sum of absolute values of percent differences between experimental and calculated vapor pressure values
DSC	differential scanning calorimetry
ECBC	U.S. Army Edgewood Chemical Biological Center
FID	flame ionization detector
GB	isopropyl methylphosphonofluoridate, sarin
GBVG	glass bead vapor generator
GC	gas chromatograph
MW	molecular weight
NBPt	normal boiling point
p	pressure (torr)
P	pressure (pascal)
P_{calc}	calculated vapor pressure
P_{exptl}	experimental vapor pressure
R	gas constant
t	temperature (Celsius)
T	temperature (kelvin)
TMoxTZ	2,4,6-trimethoxy-1,3,5-triazine
TMTZ	2,4,6-trimethyl-1,3,5-triazine
VX	*O*-ethyl-*S*-(2-diisopropylaminoethyl) methylphosphonothiolate

DISTRIBUTION LIST

The following individuals and organizations were provided with one Adobe portable document format (pdf) electronic version of this report:

U.S. Combat Capabilities Development Command Chemical Biological Center (CCDC CBC)
Chemical Analysis and Physical Properties Branch
FCDD-CBR-CP
ATTN: Ellzy, M.
Brozena, A.

CCDC CBC
CBR Filtration Branch
FCDD-CBR-PF
ATTN: Maxwell, A.
Buchanan, J.
Bruni, E.

CCDC CBC
Chemical Sciences Division
FCDD-CBR-C
ATTN: Berg, F.

Department of Homeland Security
DHS-S&T-RDP-CSAC
ATTN: Mearns, H.

CCDC CBC Technical Library
FCDD-CBR-L
ATTN: Foppiano, S.
Stein, J.

Defense Technical Information Center
ATTN: DTIC OA

Defense Threat Reduction Agency
J9-CBS
ATTN: Peacock, S.


U.S. ARMY COMBAT CAPABILITIES DEVELOPMENT COMMAND
CHEMICAL BIOLOGICAL CENTER